Phys Chem Minerals (2004) 31: 261–268
DOI 10.1007/s00269-004-0386-y

ORIGINAL PAPER

T. Okada · W. Utsumi · H. Kaneko · V. Turkevich
N. Hamaya · O. Shimomura

Kinetics of the graphite–diamond transformation in aqueous fluid determined by in-situ X-ray diffractions at high pressures and temperatures

Received: 3 March 2003 / Accepted: 2 February 2004

Abstract The graphite-diamond transformation was investigated by in situ time-resolved X-ray diffraction experiments using aqueous fluid containing dissolved MgO as the diamond-forming catalyst under conditions of 6.6–8.9 GPa and 1400–1835 °C. The transformed volume fractions of diamond as a function of time under various pressure-temperature conditions were obtained and analyzed using the JMAK rate equation. Variations in the nucleation and growth processes during diamond formation as a function of pressure and temperature were clarified.

Keywords Diamond · Kinetics · Nucleation and growth · Aqueous fluid · In situ X-ray diffraction

T. Okada (✉) · W. Utsumi · O. Shimomura
Synchrotron Radiation Research Center,
Japan Atomic Energy Research Institute,
1-1-1, Kouto, Mikazuki-cho, Sayo-gun,
Hyogo 679–5148, Japan

H. Kaneko
SPring-8 Service Co. Ltd., 2-23-1, Kouto,
Kamigori-cho, Ako-gun,
Hyogo 678–1205, Japan

V. Turkevich
Institute for Superhard Materials of the National
Academy of Sciences of Ukraine, 2,
Avtozavodskaya St., Kiev 04074,
Ukraine

N. Hamaya
Graduate School of Humanities and Sciences,
Ochanomizu University, 2-1-1, Otsuka,
Bunkyo-ku, Tokyo 112–8610,
Japan

Present address: T. Okada
Department of Earth and Space Science,
Graduate School of Science, Osaka University,
1-1, Machikaneyama-cho, Toyonaka,
Osaka 560–0043, Japan
e-mail: okataku@ess.sci.osaka-u.ac.jp
Tel.: +81-6-6850-5794
Fax: +81-6-6850-5480

Introduction

Natural diamonds are important sources of information for investigating the structure and evolution of the Earth. Although various scenarios for diamond formation have been suggested on the basis of inclusions and isotopic data (e.g. Richardson et al. 1984; Meyer 1985; Haggerty 1986; Griffin et al. 1992), these models are still debatable. Recent high-pressure experiments have demonstrated that water in a supercritical state (Yamaoka et al. 1992, 2000; Hong et al. 1999), C–O–H fluids (Akaishi and Yamaoka 2000; Shaji Kumar et al. 2000; Akaishi et al. 2000), volatile-rich silicate melt (Arima et al. 1993), and carbonate fluids (Pal'yanov et al. 1999) have catalytic effects on diamond formation. These experimental simulations may provide some insight on natural diamond formation, but they cannot elucidate the mechanism of formation because they were based on quenching methods: diamonds synthesized at high pressures and temperatures were quenched to ambient conditions and the recovered products were then examined. Direct observations are required to clarify the mechanism of diamond formation.

One powerful method for direct observation under high pressure—high temperature conditions is in situ X-ray diffraction using synchrotron radiation. Many studies have examined the kinetics of solid-solid transformations under high pressures using time-resolved X-ray diffraction techniques with synchrotron radiation (e.g., Hamaya and Akimoto 1981; Hamaya et al. 1985; Rubie et al. 1990; Rubie and Ross 1994; Nagai et al. 1997, 1998; Kubo et al. 1998, 2002). However, there have been few attempts to apply this technique to the study of diamonds. Several papers have been reported using metal catalysts (Yamaoka et al. 1985; Solozhenko et al. 2002; Turkevich et al. 2002), but none have been reported using a candidate material simulating mantle fluids because more severe experimental conditions are required. After improving the experimental technique, we have succeeded in real-time observation of the

graphite-diamond transformation in a supercritical aqueous fluid. The initial data was published in our previous papers (Okada et al. 2002a, b). We now report a series of experiments under varying pressures between 6.6 and 8.9 GPa and temperatures between 1400–1835 °C. The obtained kinetic data was analyzed based on the JMAK rate equation. The pressure–temperature dependence of spontaneous nucleation and growth processes during diamond formation is discussed.

Experimental

Experiments were carried out using a 180-ton DIA-type cubic-anvil apparatus, SMAP-2, installed on the beamline BL14B1 at the SPring-8, a third-generation synchrotron radiation facility in Harima Science Garden City, Japan (Utsumi et al. 1998, 2002). Six tungsten carbide anvils with 4-mm edges were used to generate pressure. A mixture of boron and epoxy resin was used as the pressure medium (7-mm cube) while cylindrical graphite was used as the furnace in conjunction with a molybdenum electrode. The furnace was surrounded by a $LaCrO_3$ tube, which served as a thermal insulator. Due to the large absorption of $LaCrO_3$, X-rays had difficulty passing through the insulator. To remedy this situation, small holes, which were filled with semisintered MgO rods, were made along the X-ray path. The starting material was finely powdered brucite [$Mg(OH)_2$: reagent grade, Wako Pure Chemical Industries, Ltd.] mixed with a fine graphite powder (spectroscopic grade, Nippon Carbon Co. Ltd.) in a 1:1 weight ratio. The graphite to diamond conversion process occurred in aqueous fluid containing dissolved MgO, which was formed by the decomposition of brucite at high pressure and temperature (Okada et al. 2002a). The starting material was compacted into a disk shape and packed into a cylindrical molybdenum capsule, which was covered with molybdenum inner caps on both ends to prevent the volatile components from leaking. Molybdenum was used because it does not act as a diamond-forming catalyst (Akaishi and Yamaoka 2000). Using this cell assembly, we had previously confirmed the reversible reaction between melting and solidification of brucite without formation of periclase at around 1100 °C and 6.2 GPa (Okada et al. 2002a), suggesting the adequate containment of fluid in the molybdenum capsule without serious leakage. A fine powder mixture of NaCl and hexagonal BN (3:7 by weight) was placed close to the capsule to serve as a pressure standard. The temperature was monitored by a W97Re3-W75Re25 thermocouple covered with an Al_2O_3 tube.

In situ X-ray observations were performed by energy-dispersive powder diffraction using white X-ray s provided by a bending magnet source. The incident beam was collimated to 0.05 mm in height and 0.3 mm in width. A pure Ge solid-state detector fixed at a constant 2θ angle (6.0°) collected the X-rays that were diffracted by the sample. Using this optical system, the glancing area was approximately 1 mm (length) × 0.3 mm (width) × 0.05 mm (height). Pressure was calculated from the lattice constants of NaCl using the Decker scale (Decker 1971). When direct pressure determination was difficult due to grain growth or melting of NaCl at very high temperatures, the pressure was estimated by extrapolation from lower temperature values. Pressure was first increased at room temperature, and then the temperature was increased at a rate of 100 °C min^{-1} at a constant applied load. Once the target temperature was reached, the time-resolved X-ray diffraction pattern was collected every 10 s. It is known that compression causes strain in the sample, which greatly affects the kinetics of transformation; annealing the sample at high temperature is important to remove this strain (Rubie et al. 1990). In this study, however, transformation occurred in aqueous fluid; therefore, the strain in the graphite had already been released.

The products of each run were recovered and treated with sulfuric acid for approximately 10 min to remove the catalyst (recrystallized brucite and periclase). Then the products were investigated using a scanning electron microscope equipped with an energy-dispersive spectrometer (SEM-EDS).

Results and discussion

Transformation rates

Figure 1 plots the experimental P–T conditions together with the graphite-diamond equilibrium curve (Kennedy and Kennedy 1976) and the mantle geotherm (Jeanloz and Morris 1986). As in our previous study (Okada et al. 2002a), the brucite melted completely under these P–T conditions without the crystallization of periclase or other carbonates such as magnesite. Thus, aqueous fluid containing dissolved MgO, which was formed by the melting of brucite, played a catalytic role in the graphite-diamond transformation. (The experimental conditions used were not high enough to allow the direct conversion of graphite to diamond without catalysts (Wentorf 1966; Akaishi et al. 1990). Figure 2 shows a typical series of diffraction patterns during the transformation at 8.8 GPa and 1450 °C (run 6). Under this condition, diamond diffraction peaks first appeared 440 s after the target temperature, 1450 °C, was reached, which implies that 440 s of incubation time was necessary for spontaneous diamond nucleation. As the time increased, the intensity of the graphite 002 diffraction line decreased, while the intensity of the diamond 111 diffraction line increased.

For the kinetic analyses, the transformed volume fractions as a function of time were calculated. It was

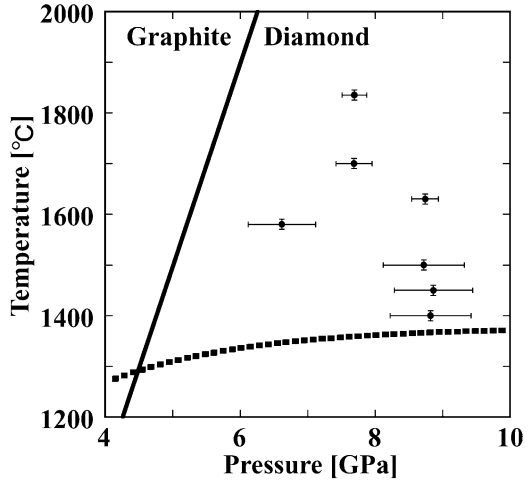

Fig. 1 A pressure–temperature diagram depicting the experimental conditions. The *solid curve* is the equilibrium boundary between graphite and diamond determined by Kennedy and Kennedy (1976). The *dotted curve* is the mantle geotherm estimated by Jeanloz and Morris (1986). The relationship between monitored pressure and temperature up to 1000 °C was fitted using a linear equation. The pressures at the desired temperatures were estimated by extrapolation. The estimated errors in pressure are expressed as the computational errors in the fittings. The estimated errors in temperature are based on the finite difference calculation by Turkevich et al. (2002)

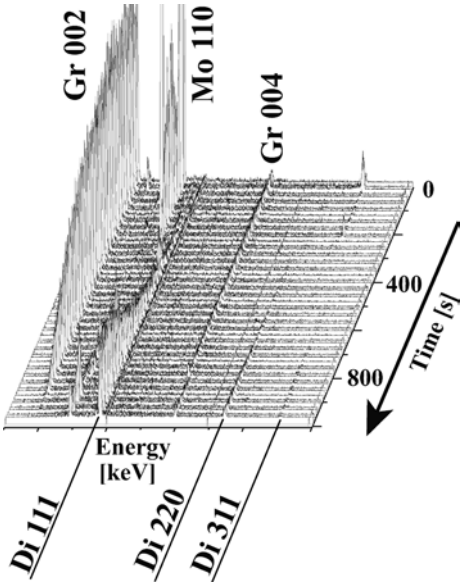

Fig. 2 Variations of the sample diffraction patterns during the graphite-diamond transformation at 8.9 GPa and 1450 °C (run 6). The profiles were consecutively recorded every 10 s. Gr, Mo and Di denote the diffraction lines of graphite, molybdenum (capsule) and diamond, respectively. The intensity of the graphite peak wa s clearly reduced while the diamond peak increased, reflecting the amount of diamond present

assumed that the relative integrated intensities of the diffraction peaks were proportional to the volume fraction of each phase because the X-ray absorption coefficient of the sample remained constant during the transformation. The diffraction peaks of 002 in graphite and 111 in diamond were used to estimate the volume fractions of each phase since these reflections were the most intense. Since we prioritized acquisition of a profile in a short exposure time, the other small peaks did not have high enough intensity or quality for kinetic analysis. The integrated intensities were calculated by fitting the diffraction peaks with Gaussian functions. We estimated the transformed volume fraction of graphite (ζ^{Gr}) and diamond (ζ^{Di}) from the integrated intensities of graphite (I^{Gr}) and diamond (I^{Di}) relative to the integrated intensity of graphite before the transformation ($I^{Gr}_{100\%}$) and of diamond after the transformation ($I^{Di}_{100\%}$), respectively (Kubo et al. 1998, 2002).

$$\zeta^{Gr} = \frac{I^{Gr}}{I^{Gr}_{100}\%} \tag{1}$$

$$\zeta^{Di} = \frac{I^{Di}}{I^{Di}_{100}\%} \tag{2}$$

The average of the transformed volume fractions (ζ^{ave}) calculated from the graphite and diamond peaks was defined as the real transformed volume fraction (ζ).

$$\zeta \equiv \zeta^{ave} = \frac{(1-\zeta^{Gr}) + \zeta^{Di}}{2} \tag{3}$$

Figure 3 shows the variations in transformed volume fraction (ζ) with time. The error bars show the standard deviations of the averages. The large errors at 7.7 GPa were caused by the uncertain intensities of diamond diffraction peaks due to the existence of large crystals and their preferred orientation. Figure 3 indicates that at a constant pressure, longer incubation times were required for spontaneous diamond nucleation and slower transformation rates were observed with decreasing temperatures. At 6.6 GPa and 1580 °C (run 3), and 8.8 GPa and 1400 °C (run 7), diamond was not formed in the initial 2 h, which suggests that the incubation time for spontaneous diamond nucleation was longer than 2 h.

Figure 4 plots the required times for diamond transformations under various P–T in a time–temperature–transformation (TTT) diagram, which describes the progress of a transformation with temperature and time. The time required to achieve 10% completion of the transformation was estimated from Fig. 3. These experimental data indicate that the transformation time decreased with increasing temperature. However, it is known that TTT curves have a C-shape when the high-temperature stable phase transforms into the low-temperature stable phase at a temperature lower than the equilibrium condition. The transformation rate is slow at very low temperatures and increases with increasing temperature, but at a certain temperature this trend reverses and longer transformation times are needed as

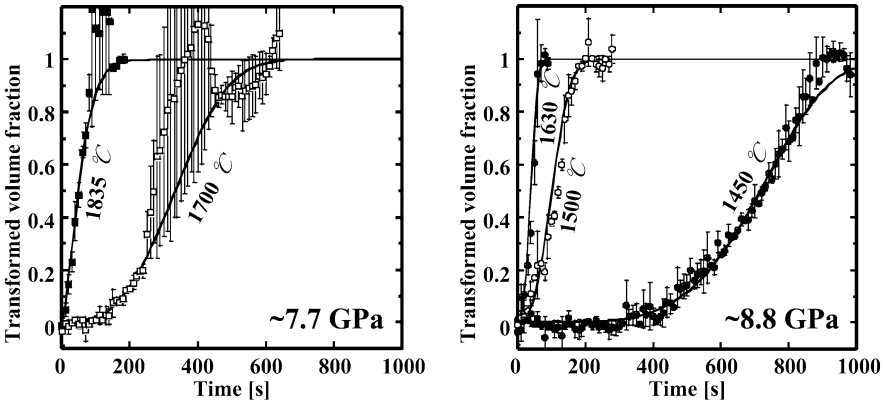

Fig. 3 Transformed volume fractions of diamond as a function of time at various pressures and temperatures. At identical pressures, longer incubation times are required for spontaneous diamond nucleation and slower transformation rates are observed with decreasing temperature. The *solid curves* are best-fit curves generated by least–squares fitting of the JMAK rate equation to the experimental data

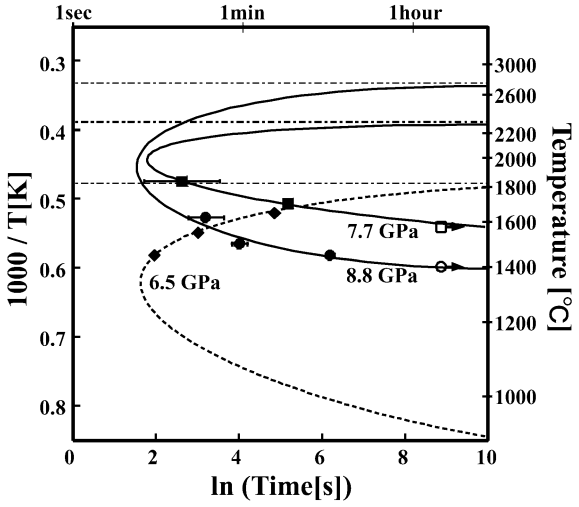

Fig. 4 Time-temperature-transformation (TTT) diagram of graphite–diamond transformation. Times required to complete 10% of the diamond transformation are plotted against temperature. ■ and ● denote the data acquired at ~7.7 GPa and ~8.8 GPa, respectively. □→ and ○→ indicate that in 2 h there was no diamond transformation at this temperature. *Solid curves* are the schematic TTT curves at each pressure, which should be asymptotic to the graphite–diamond equilibrium temperatures (*dot-dashed lines* 2304 °C at 7.7 GPa and 2744 °C at 8.8 Gpa: Kennedy and Kennedy 1976). ◆ denotes the results by Turkevich et al. (2002) using Fe–Al alloy as a catalyst; the speculative TTT curve from this experiment is also shown as a *dashed curve*

the temperature approaches equilibrium. The solid curves in Fig. 4 are the speculative whole TTT curves. The experimental data from this study is located on the low-temperature side of the C-shaped curve. Unfortunately, due to technical difficulties, data could not be directly obtained for the high-temperature side of the C-shaped curve. Turkevich et al. (2002) conducted a similar experiment using Fe–Al metal alloy as a diamond-forming catalyst in the same facility that was used for this study. As a reference, their results are also plotted in Fig. 4. In the Turkevich study, the transformation time increased with increasing temperature, which indicates that their data was collected on the high-temperature side of the TTT curve (a dotted curve).

In these experiments, the temperature was not directly jumped to the target temperature but was increased at a rate of 100 °C min^{-1} because a temperature jump at high pressure is technically difficult due to the risk of a blow out of the high-pressure cell. Therefore, there were time intervals before the temperature reached the target value, which might affect the transformation rate, particularly the incubation time. We believe that this effect is small even in these experiments for the following reason. Solid-phase brucite has no catalytic effect on diamond formation. Thus, the time interval prior to the decomposition of brucite at around 1100 °C does not affect the kinetics of diamond transformation. The time interval between 1100 °C and the target temperatures was 3–7 min, which might influence the conclusions of the kinetic analysis. However, we confirmed that diamond formation did not occur after a 2-h incubation at comparatively low temperatures (1580 °C at 6.6 GPa and 1400 °C at 8.8 GPa). This suggests that the time interval required to pass through the higher temperatures that may have a great influence on the transformation rate is only 0.5–2.5 min. The effect of such a short interval on the conclusions of the analysis is probably negligible, although it is formally possible that the incubation time is slightly underestimated.

Nucleation and growth processes

The JMAK rate Eq. (4), which is based on a statistical model, was originally formulated by Johnson and Mehl (1939), Avrami (1939, 1940, 1941) and Kolmogorov (1937), and describes the relationship between time and the transformed volume fraction.

$$\zeta = 1 - \exp(-k \cdot t^n) \quad \text{or} \quad \ln\ln\left(\frac{1}{1-\zeta}\right) = \ln k + n \ln t \ , \tag{4}$$

where ζ is the transformed volume fraction, k is the rate constant, t is time and n is a constant that depends on the reaction mechanism. Table 1 categorizes the n values in the JMAK rate equation by conditions for the nucleation and growth processes according to Christian (1965). The ζ-time data were fitted to the JMAK rate equation using a weighted non-linear least-squares procedure. The values of n and k were optimized to minimize the chi-square (χ^2_{min}) of the fit. Figure 3 shows the fitted curves and Table 2 summarizes the estimated values of n and k. The approximate n values that best described the experimental ζ-time data were n ≈ 1.5 (run 1: 1835 °C at ~7.7 GPa), $n \approx 3$ (run 2:1700 °C at ~7.7 GPa, run 4: 1630 °C at ~8.8 GPa and run 5: 1500 °C at ~8.8 GPa), $n \approx 5$ (run 6:1450 °C at ~8.8 GPa). Using the Christian model (Christian 1965), the n values obtained in these experiments were characterized by following the nucleation and growth processes. In run 1, $n \approx 1.5$ indicates that instantaneous nucleation of diamonds occurred and that the growth process was controlled by carbon diffusion to the surfaces of the growing crystals. In runs 2, 4 and 5, where n is

Table 1 n values in the JMAK rate equation according to the combination of nucleation and growth processes categorized by Christian (1965)

	Growth Process	
	Interface-controlled Growth	Diffusion-controlled Growth
Nucleation Process		
Instantaneous nucleation	3	1.5
Constant nucleation rate to time	4	2.5
Increasing nucleation rate with time	>4	>2.5

Table 2 Experimental conditions, calculated kinetic parameters and estimated nucleation and growth processes

Run	T(°C)	P (Gpa)	Overpressure (Gpa)[a]	n[b]	k (s^{-n})[b]	Estimated nucleation and growth process[c]
1	1835	7.7	1.8	1.5	2.0×10^{-3}	Instantaneous nucleation and diffusion controlled growth ($n = 1.5$)
2	1700	7.7	2.2	3.1	1.1×10^{-8}	Instantaneous nucleation and interface-controlled growth ($n = 3$) or (Increasing nucleation rate and diffusion controlled growth ($n > 2.5$))
3	1580	6.6	1.4	(No transformation for 2 h)		
4	1630	8.7	3.4	3.2	3.7×10^{-6}	(Instantaneous nucleation and interface-controlled growth ($n = 3$)) or Increasing nucleation rate and diffusion-controlled growth ($n > 2.5$)
5	1500	8.7	3.7	2.9	9.2×10^{-7}	(Instantaneous nucleation and interface-controlled growth ($n = 3$)) or Increasing nucleation rate and diffusion-controlled growth ($n > 2.5$)
6	1450	8.9	4.0	5.1	1.9×10^{-15}	Increasing nucleation rate and interface-controlled growth ($n > 4$) or Increasing nucleation rate and diffusion-controlled growth ($n > 2.5$)
7	1400	8.8	4.1	(No transformation for 2 h)		

[a] Overpressure was estimated based on the equilibrium boundary by Kennedy and Kennedy (1976)

[b] Values of n and k were calculated by least-squares fits of the obtained kinetic data using the JMAK rate equation

[c] Probable processes of nucleation and growth were estimated based on the obtained n values. The process in parentheses is less probable based on the SEM observations

approximately 3, the process is characterized either by ''instantaneous nucleation and interface-controlled growth (n=3)'' or by ''an increasing nucleation rate with time and diffusion-controlled growth ($n > 2.5$).'' For run 6 ($n \approx 5$) the process is either ''an increasing nucleation rate and interface-controlled growth ($n > 4$)'' or ''an increasing nucleation rate and diffusion-controlled growth ($n > 2.5$).''

To further restrict the $n \approx 3$ and $n \approx 5$ cases, SEM observations of the recovered diamond samples were analyzed (Fig. 5). The SEM images were classified into two groups according to the number of nuclei and the grain size. The diamonds recovered from ~7.7 GPa (Fig. 5 a run 1, 1835 °C and b run 2, 1700 °C) were characterized by large grain size (>5 μm) and small number of nuclei. The diamonds recovered from ~8.8 GPa (Fig.5 c run 4, 1630 °C, d run 5, 1500 °C, and e run 6,1450 °C) were characterized by small grain size (1–2 μm) and large number of nuclei. Variations in the nucleation process are thought to cause the different numbers of nuclei. If, in the initial stage, nucleation occurs instantaneously, then the number of nuclei will be relatively small and the diamonds will grow to a comparatively larger size. On the other hand, if nucleation occurs continuously and the nucleation rate increases with time, then the number of nuclei will be comparatively large and the grain size will be relatively small. After analyzing both the JMAK rate equation and the SEM observations, the following conclusions were drawn. Run 2 demonstrated ''instantaneous nucleation and interface-controlled growth.'' Run 4 and run 5 showed an ''increasing nucleation rate with time and diffusion-controlled growth.'' The amount of nucleation is also thought to depend on the pressure difference (overpressure, ΔP) between the equilibrium pressure of the graphite–diamond boundary and the experimental conditions; ΔP provides a driving force ($\Delta G = \Delta V \Delta P$) to overcome the nucleation barrier for transformation to occur. When ΔP becomes larger, the number of nuclei should increase. The SEM observations in Fig. 5 are also consistent with this hypothesis.

We were not able to judge the growth process for run 6 (8.8 GPa, 1450 °C) by this method. Although both the n value from JMAK analysis and the SEM observations suggest an ''increasing nucleation rate with time'', we cannot conclude experimentally whether the growth process was ''diffusion-'' or ''interface-'' controlled. However, in a manner analogous to the growth process at ~7.7 GPa, which changed from ''diffusion-controlled growth'' to ''interface-controlled growth'' with decreasing temperature, it is likely that run 6 should be categorized as an ''increasing nucleation rate with time and interface-controlled growth.''

The estimated general tendency of the growth process is summarized in the TTT diagram in Fig. 6. At low temperatures, the diamond growth process is interface-controlled; however, diffusion-controlled growth becomes dominant as the temperature approaches the nose of the TTT curve. As the temperature approaches the graphite–diamond equilibrium temperature, interface-controlled growth again becomes dominant. We were unable to directly obtain experimental data on the high-temperature side of the C-shaped TTT curve, but Turkevich et al. (2002) confirmed the high-temperature side of the curve in their experiments with the Fe–Al catalyst. The relationship between the diffusion rate and

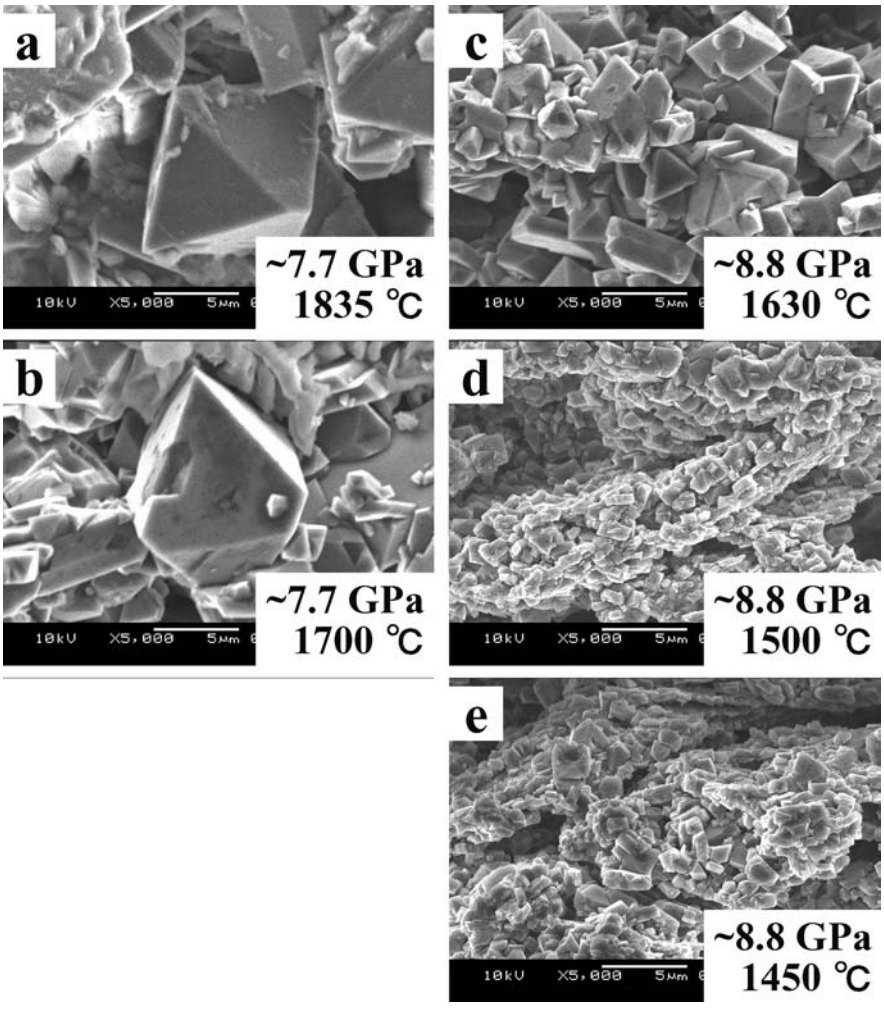

Fig. 5 SEM images of the recovered diamond specimens after treatment with sulfuric acid

the interface condition should determine the growth process. The diffusion rate of carbon increases monotonously with temperature, but the rate of capture of carbon onto the diamond surface reaches a maximum point at a certain temperature. In the mid-temperature region, the capture rate of carbon is higher than the carbon diffusion rate, making the process "diffusion-controlled growth."

The empirical activation energy can be estimated from the TTT curve when the same mechanism governs the kinetics at various temperatures. Using the "time to a given fraction" method (Putnis 1992), the time t_Y to transform a given fraction $\zeta = Y$ is given by Eq. (5).

$$\ln t_Y = \text{const} + \frac{E_a}{RT} \tag{5}$$

where E_a is the empirical activation energy for the reaction, R is the ideal gas constant, and T is the absolute temperature. From the above discussion, it is assumed that the same mechanism governs the kinetics in runs 4 and 5. Under these two conditions, the fitted straight line yields an activation energy of 174 kJ mol^{-1}. The flatter slope of the TTT curve in the lower–temperature region suggests that the activation energy for nucleation increased with decreasing temperature, which resulted in a longer incubation time for spontaneous nucleation.

Conclusions

Time-resolved X-ray diffraction experiments were performed to examine the graphite-diamond transformation in aqueous fluid under conditions of 6.6–8.9 GPa and 1400–1835 °C. The transformed volume fractions of diamond as a function of time under various pressure-temperature conditions were obtained. By analyzing the kinetic data using the JMAK rate equation and SEM images of the run products, it was determined that altering the pressure–temperature conditions drastically changes the nucleation and growth processes of diamond.

The time-temperature-transformation (TTT) diagram is useful in estimating the time required for diamonds to form naturally. According to Haggerty et al. (1986), the estimated conditions for diamonds to form naturally in the Earth are about 5–6 GPa and 900–1400 °C, which is much lower than the conditions used

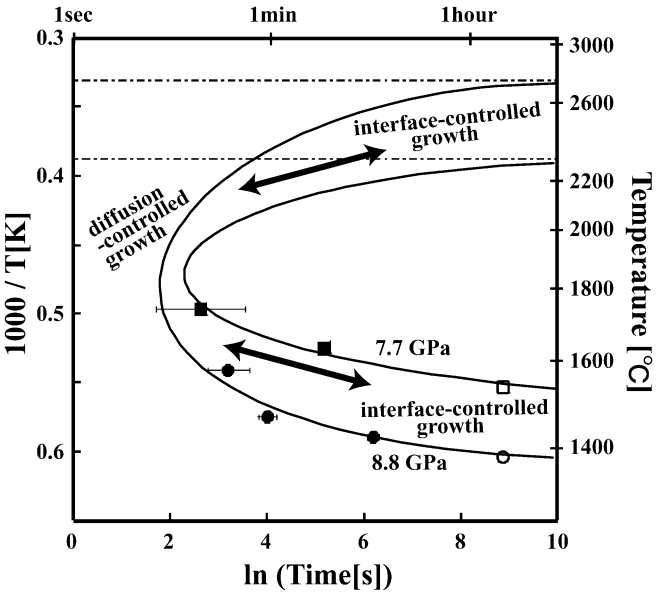

Fig. 6 General tendencies of the diamond growth process under various pressure–temperature conditions. At low temperatures the diamond growth process is interface-controlled. As the temperature approaches the nose of the TTT curve, diffusion-controlled growth becomes dominant. When the temperature moves towards the graphite-diamond equilibrium temperature, interface-controlled growth is again dominant

in this study. The TTT curve for this condition must lie below the equilibrium temperature (1224° C at 5 GPa and 1624°C at 6 GPa (Kennedy and Kennedy 1976)) and shifts towards the right (in the direction of longer time) in Fig. 6. By accumulating more data points, using this technique together with quenching experiments, the time needed to form natural diamond under these conditions will be more precisely determined.

In this study, the system was simplified by using aqueous fluid containing dissolved MgO as a diamond forming catalyst. Even though mantle fluids and/or silicate melts, which could play a catalytic role in natural diamond formation, must have much more complicated composition, we believe that our experimental method is an important advance for detailed studies of the diamond formation process in the Earth. Further studies investigating the effects of the catalytic composition on the mechanisms of diamonds formation and the reaction time are underway.

Acknowledgements We are grateful to Drs. Y. Katayama, K. Funakoshi, Y. Nishihata, T. Katsura, T. Nagai and T. Kubo for their support in the experiments and valuable discussions. Critical reviews by two anonymous referees were helpful in improving the manuscript.

References

Akaishi M, Yamaoka S (2000) Crystallization of diamond from C-O-H fluids under high-pressure and high-temperature conditions. J Cryst Growth 209: 999–1003

Akaishi M, Kanda H, Yamaoka S (1990) High–pressure synthesis of diamond in the systems of graphite–sulfate and graphite–hydroxide. Jpn J Appl Phys 29: L1172-L1174

Akaishi M, ShajiKumar MD, Kanda H, Yamaoka S (2000) Formation process of diamond from supercritical H_2O–CO_2 fluid under high–pressure and high–temperature conditions. Diamond Relat Mater 9: 1945–1950

Arima M, Nakayama K, Akaishi M, Yamaoka S, Kanda H (1993) Crystallization of diamond from a silicate melt of kimberlite composition in high-pressure and high-temperature experiments. Geology 21: 968–970

Avrami M (1939) Kinetics of phase change. I. General theory. J Chem Phys 7: 1103–1112

Avrami M (1940) Kinetics of phase change. II. Transformation-time relations for random distribution of nuclei. J Chem Phys 8: 212–224

Avrami M (1941) Kinetics of phase change. III. Granulations, phase change, and microstructure. J Chem Phys 9: 177–184

Christian JW (1965) Phase transformations. In: Cahn RW (ed) Physical metallurgy. North-Holland, Amsterdam, pp 471–587

Decker DL (1971) High-pressure equation of state for NaCl, KCl, and CsCl. J Appl Phys 42: 3239–3244

Griffin WL, Gurney JJ, Ryan CG (1992) Variations in trapping temperatures and trace elements in peridotite-suite inclusions from African diamonds: evidence for two inclusion suites, and implications for lithosphere stratigraphy. Contrib Mineral Petrol 110: 1–15

Haggerty SE (1986) Diamond genesis in a multiply-constrained model. Nature 320: 34–38

Hamaya N, Akimoto S (1981) Kinetics of pressure-induced phase transformation in KCl at room temperature. High Temp High Press 13: 347–358

Hamaya N, Yagi T, Yamaoka S, Shimomura O, Akimoto S (1985) Time-resolved X-ray diffraction analysis of the phase transition in BaS at high pressures and high temperatures. In: Minomura S (ed) Solid state physics under pressure. KTK Scientific, Tokyo, pp 357–362

Hong SM, Akaishi M, Yamaoka S (1999) Nucleation of diamond in the system of carbon and water under very high pressure and temperature. J Cryst Growth 200: 326–328

Jeanloz R, Morris S (1986) Temperature distribution in the crust and mantle. Ann Rev Earth Planet Sci 14: 377–415

Johnson WA, Mehl RF (1939) Reaction kinetics in processes of nucleation and growth. Trans Am Inst Min Met Eng 135: 416–442

Kennedy CS, Kennedy GC (1976) Equilibrium boundary between graphite and diamond. J Geophys Res 81: 2467–2470

Kolmogorov AN (1937) Statistical theory of nucleation processes. Izv Acad Nauk SSSR Ser Math 3: 355–366

Kubo T, Ohtani E, Kato T, Morishima T, Yamazaki D, Suzuki A, Mibe K, Kikegawa T, Shimomura O (1998) An in situ X–ray diffraction study of the α–β transformation kinetics of Mg_2SiO_4. Geophys Res Lett 25: 695–698

Kubo T, Ohtani E, Kato T, Urakawa S, Suzuki A, Kanbe Y, Funakoshi K, Utsumi W, Kikegawa T, Fujino K (2002) Mechanisms and kinetics of the post-spinel transformation in Mg_2SiO_4. Phys Earth Planet Inter 129: 153–171

Meyer HOA (1985) Genesis of diamond: a mantle saga. Am Mineral 70: 344–355

Nagai T, Ohtaka O, Yamanaka T (1997) Kinetic studies of the α-quartz-coesite transformation of SiO_2. Mineral J 19: 147–154

Nagai T, Mori S, Ohtaka O, Yamanaka T (1998) Nucleation and growth kinetics of the α-quartz-coesite transformation using both powder and single crystal samples. Rev High Pressure Sci Technol 7: 125–127

Okada T, Utsumi W, Kaneko H, Yamakata M, Shimomura O (2002a) In situ X-ray observations of the decomposition of brucite and the graphite-diamond conversion in aqueous fluid at high pressure and temperature. Phys Chem Miner 29: 439–445

Okada T, Utsumi W, Shimomura O (2002b) In situ x-ray observations of the diamond formation process in the C–H_2O–MgO system. J Phys Condens Matter 14: 11331–11335

Pal'yanov YN, Sokol AG, Borzdov YM, Khokhryakov AF, Sobolev NV (1999) Diamond formation from mantle carbonate fluids. Nature 400: 417–418

Putnis A (1992) Introduction to mineral sciences. Cambridge University Press, Cambridge

Richardson SH, Gurney JJ, Erlank AJ, Harris JW (1984) Origin of diamonds in old enriched mantle. Nature 310: 198–202

Rubie DC, Ross CR (1994) Kinetics of olivine-spinel transformation in subducting lithosphere: experimental constraints and implications for deep slab processes. Phys Earth Planet Inter 86: 223–241

Rubie DC, Tsuchida Y, Yagi T, Utsumi W, Kikegawa T, Shimomura O, Brearley AJ (1990) An in situ X ray diffraction study of the kinetics of the Ni_2SiO_4 olivine–spinel transformation. J Geophys Res 95: 15829–15844

ShajiKumar MD, Akaishi M, Yamaoka S (2000) Formation of diamond from supercritical H_2O–CO_2 fluid at high pressure and high temperature. J Cryst Growth 213: 203–206

Solozhenko VL, Turkevich VZ, Kurakevych OO, Crichton WA, Mezouar M (2002) Kinetics of diamond crystallization from the melt of the Fe–Ni–C system. J Phys Chem B 106: 6634–6637

Turkevich V, Okada T, Utsumi W, Garan A (2002) Kinetics of diamond spontaneous crystallization from the melt of the Fe–Al–C system at 6.5 GPa. Diamond Relat Mater 11: 1769–1773

Utsumi W, Funakoshi K, Urakawa S, Tsuji K, Konishi H, Shimomura O (1998) SPring-8 beamline for high pressure science with multi-anvil apparatus. Rev High Pressure Sci Technol 7: 1484–1486

Utsumi W, Funakoshi K, Katayama Y, Yamakata M, Okada T, Shimomura O (2002) High-pressure science with a multi-anvil apparatus at SPring-8. J Phys Condens Matter 14: 10497-10504

Wentorf Jr. RH (1966) Solutions of carbon at high pressure. Ber Bunsenges Phys Chem 70: 975–982

Yamaoka S, Akaishi M, Kanda H, Osawa T (1992) Crystal growth of diamond in the system of carbon and water under very high pressure and temperature. J Cryst Growth 125: 375-377

Yamaoka S, ShajiKumar MD, Akaishi M, Kanda H (2000) Reaction between carbon and water under diamond-stable high pressure and high temperature conditions. Diamond Relat Mater 9: 1480–1486

Yamaoka S, Shimomura O, Yagi T, Akimoto S (1985) Direct observation of the conversion reaction from graphite to diamond. In: Minomura S (ed) Solid state physics under pressure. KTK Scientific, Tokyo, pp 369–374